Available online at www.sciencedirect.com
SciVerse ScienceDirect
Physics Procedia 40 (2013) 45 – 48
Physics Procedia

2nd European Conference on Nano Films: ECNF-2012

SAXS Investigation on the Fractal Properties of MnO_2 Semiconductor Thin Films

Leonid Skatkov[a], Valeriy Gomozov[b,a] *

[a]*PCB "Argo", 4/23 Shaul ha-Melekh Street, 84797 Beer Sheva, Israel*
[b]*NTU"KhPI", 21 Frunze Street, 61002 Kharkov, Ukraine*

Abstract

This paper presents the results of investigations on the morphology and porous concentration distribution in the MnO_2 and also the fractal properties of porous semiconductor. The volume fractal dimension are stated to be order 2.9 which is a stipulation of a highly developed porous structure of MnO_2. The present results provide experimental support to the theory developed earlier.

Selection and/or peer-review under responsibility of VINF.
Keywords: pore, X-ray scattering, fractal dimension, films

1.Experimental

Porous films have been prepared by the thermal deposition (pyrolysis) of $Mn(NO_3)_2$ under the temperature T=570K according with reaction of pyrolysis (1):

$$Mn(NO_3)_2 \times 6H_2O = MnO_2 + 2NO_2 + 6H_2O \qquad (1)$$

The nature of angular distribution, asymptotes, and integral parameters , invariants, of the small-angle X-ray scattering (SAXS) indicatrixes, which were used to determine the morphology of the electron density scattering inhomogeneities (pores) were analysed. Surface microrelief of MnO_2 were investigated by OLYMPUS SZX12 optical microscope.

*Leonid Skatkov. Tel.: +972 8 648 2255; fax: +972 8 640 1754
E-mail address: sf_lskatkov@bezeqint.net

Selection and/or peer-review under responsibility of VINF
doi:10.1016/j.phpro.2012.12.006

2. Results and Discussion.

2.1. Porous structure.

The morphology, concentration and size distribution of MnO_2 have been investigated by SAXS. The observed SMPs were in the range $0,1 \le 2R \le 100$nm. We've analyzed the following values: type of angular distribution; asymptotics and the integral parameters of the dispersion indices of SAXS related to the typical size l_n; the typical volume V_n and the typical SMP shadow area f_n. The mean square size of the SMP has been determined by the tangent technique described in by Kratky [1].
Since the size distribution appeared to be polymodal, we've divided the pores into four groups, according to their size: $2R \le 1$nm; $1\text{nm} \le 2R \le 4$nm; $4\text{nm} \le 2R \le 8$nm; $8\text{nm} \le 2R \le 50$nm.

The absence of noticeable anisotropy of SAXS shows the character of the dispersion indices which asymptotically comply with the Porod law $I(s) \sim s^{-4}$ (where I(s) is the intensity of X-ray and s is a diffraction vector). One can assume that scattering SMPs have no domineering orientation, and they are more equiaxial than macro- and micropores. However, some differences in the integral parameters l_n = 5nm; $V_n^{1/3}$ = 5nm and $f^{1/2}$ =13nm allows us to conclude that SMP axes are quite equal. Absolute values of these are close to the values calculated by the Guinier technique based on another way of averaging pore sizes. This affirms that most SMPs have more or less equal axes, unlike macropores.

As it can be seen from the Tab.1 the major contribution to the SMP volume concentration is made by submicropores not exceeding 8 nm – mostly from the range of $1 \le 2R \le 8$nm. The total share of the SMPs in the MnO_2 film is about 9.8 % which conforms to the known value [2].

Table 1. Characteristics of submicropores in MnO_2.

Square average size of SMP's (nm)	Volume concentration of SMP (%)	Quantity of SMP in the scattering volume (cm^{-3})	Distance between SMP (nm)
1	1	$3x10^{15}$	3
4	4	$9x10^{13}$	9
8	4,6	$1x10^{13}$	20
16	$1,5x10^{-3}$	$2x10^{7}$	$1,5x10^{3}$

It should be noticed that, unlike macro- and micropores, some equiaxial SMPs are closed and filled with gas. Their formation results from both clustering oxygen vacancies shaped in MnO_2 films and the fact that solidifying rate during the pyrolysis largely exceeds gas emission rate. A part of the emitted gas is therefore trapped in the SMPs.
The invariant curve of the dispersion indices (Fig.1) reflects the distribution pattern of SMP over their volumes. Here, one can see several maxima; this confirms that the distribution is polymodal, i.e. SMP exists in several typical sizes. This can be a
result of (i) peculiarities in the process of pore formation involving gases and crystals

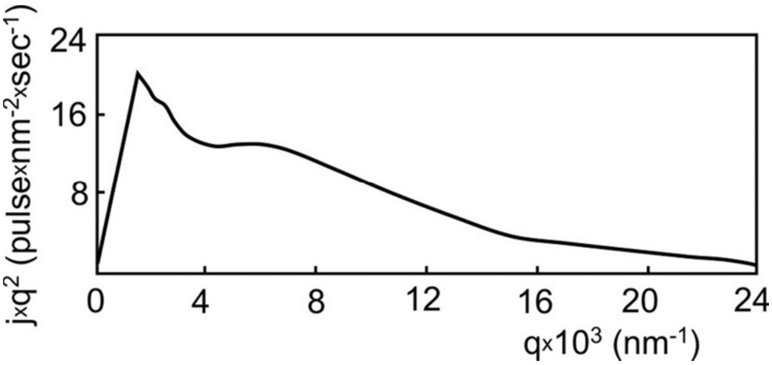

Fig. 1. Relation between SAXS indicatrix invariant, Iq^2, and diffraction vector q (I – SAXS intensity) for MnO_2.

or (ii) the process where clustering of oxygen vacancies and continuous gas evacuation in bubbles is accompanied by the growth of the 1atter. Some bubbles burst before solidifying as a result of internal pressure, but some solidify and remain in the layer. It is quite natural that families of arising, growing and bursting bubbles are described by different distribution.

2.2. Fractal properties.

The developed surface microrelief of MnO_2 films (Fig.2) contributes to interesting investigation of the fractal properties of this compound.

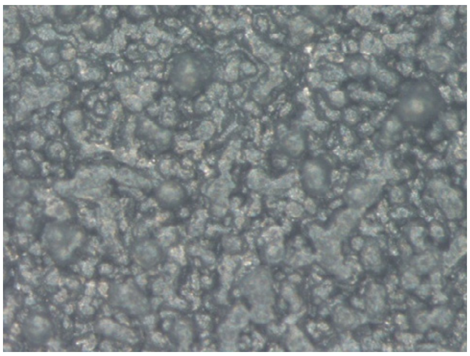

Fig. 2. Microscope image of MnO_2 surface (x90)

.

As it is known [3] in order to describe X-ray scattering by a porous solid even in the Porod region, i.e. $aq^{-1}R$ (where q is a wave vector, a is a lattice constant and R is a the largest domain size) the well known q^{-4} law must be modified. The appropriate theory was developed by Wong [4] and the main formula of this theory for scattering of surface is as follows:

$$I(q) \sim const \times q^{D-6} \qquad (2)$$

Here I(q) – is the SAXS intensity and D is the surface fractal dimension.

Calculation of I(q) – q dependencies allows to determine to which area of the object corresponds information on dispersion [5]. In case when the index value $\alpha = -\partial \lg I(q) / \partial \lg q$ is in the range of 3 – 4, the dispersion is affected by the surface area of the object and measurement results allows to determine fractal dimension of the surface D = 6 - α (for three-dimensional object $2 \leq D \leq 3$). In case when $\alpha \leq 3$, dispersion is caused with the full volume of the object, which dimension is D = α.

In our case the scattered intensity/wave vector relationship (Fig.3) shows the fractal behavior.

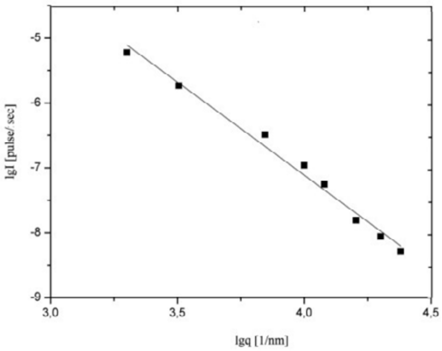

Fig.3. Logarithmic dependence of the SAXS intensity vs the wave-vector q: (■) – experimental data; (__) – approximation to the linear range.

Indeed, on the graph, the coefficient of the curved part of the slope, which can be closely approximated by the line, (Fig.3) is: α = 2.87. Consequently, considering the abovementioned the present situation contributes to dispersion with full volume of the covering while fractal dimension of MnO_2 is determined as D=α=2.87.

The received value is very close to the value of fractal dimension of sintered niobium ($D_{(Nb)}$ = 2.81) calculated in [6]. At the present time the authors can hardly say whether it is a simple coincidence or is related to special features of the structures' formation. At least, it shall be pointed that as it has been shown in [7] in case of sintered niobium fractal dispersion is caused due to the surface of the object.

References

[1] Glater,O, Kratky,O Small-Angle X- Ray scattering, Academic Press, London- New York (1982).

[2] Gomozov,V , Voskoboynikov M, Solid state electrochemistry processes under the function of Ta – Ta_2O_5 – MnO_2 capacitor structure, *Vestnik KhPI*, 246 (1987) 63.

[3] Bale,H ,.Schmidt,P Small-Angle X-Ray scattering investigation submicroscopic porosity with fractal properties, *Phys.Rev.Lett.*53 (1984) 596.

[4]. Po-zen Wong, Scattering by inhomogeneous systems with rough internal surfaces: porous solids and random- field ising systems, *Phys.Rev*., B 32 (1985) 7417.

[5] Smirnov,B.M. Physics of Fractal Aggregates, Nauka, Moscow (1991).

[6] Skatkov,L., Konotop,V., Cheremskoy P., .Gomozov,V., Bayrachny,B. Surface fractal dimension of sintered porous solid niobium, *Appl.Surf.Sci.* 81 (1994) 427.

[7] Skatkov,L., Konotop,V., Cheremskoy, P., Gomozov,v.,Bayrachny, B.,Porous solid niobium as fractal structure, *Phys.Stat.Sol.(b)* 183 (1994) K1.